Langmuir
Article
pubs.acs.org/Langmuir

Microfluidic Directed Self-Assembly of Liposome−Hydrogel Hybrid Nanoparticles

Jennifer S. Hong,*[,†,§] Samuel M. Stavis,[†] Silvia H. DePaoli Lacerda,[⊥] Laurie E. Locascio,[‡] Srinivasa R. Raghavan,[∥] and Michael Gaitan[†]

[†]*Semiconductor Electronics Division,* [‡]*Biochemical Science Division, National Institute of Standards and Technology, Gaithersburg, Maryland 20899,* [§]*Department of Bioengineering, and* [∥]*Department of Chemical and Biomolecular Engineering, University of Maryland, College Park, Maryland 20742, and* [⊥]*Center for Biologics Evaluation and Research, Food and Drug Administration, Bethesda, Maryland 20817*

Received March 2, 2010. Revised Manuscript Received April 13, 2010

We present a microfluidic method to direct the self-assembly of temperature-sensitive liposome−hydrogel hybrid nanoparticles. Our approach yields nanoparticles with structural properties and highly monodisperse size distributions precisely controlled across a broad range relevant to the targeted delivery and controlled release of encapsulated therapeutic agents. We used microfluidic hydrodynamic focusing to control the convective-diffusive mixing of two miscible nanoparticle precursor solutions (a DPPC:cholesterol:DCP phospholipid formulation in isopropanol and a photopolymerizable *N*-isopropylacrylamide mixture in aqueous buffer) to form nanoscale lipid vesicles with encapsulated hydrogel precursors. These precursor nanoparticles were collected off-chip and were irradiated with ultraviolet (UV) light in bulk to polymerize the nanoparticle interiors into hydrogel cores. Multiangle laser light scattering in conjunction with asymmetric flow field-flow fractionation was used to characterize nanoparticle size distributions, which spanned the ≈150 to ≈300 nm diameter range as controlled by microfluidic mixing conditions, with a polydispersity of ≈3% to ≈5% (relative standard deviation). Transmission electron microscopy was then used to confirm the spherical shape and core−shell composition of the hybrid nanoparticles. This method may be extended to the directed self-assembly of other similar cross-linked hybrid nanoparticle systems with engineered size/structure−function relationships for practical use in healthcare and life science applications.

Introduction

Soft nanoparticles such as nanoscale lipid vesicles, hydrogel nanoparticles, and hybrids of the two have many important applications in healthcare and the life sciences.[1,2] Such nanoparticles have been applied in areas of single molecule manipulation and metrology,[3] sensors,[4] biomedical imaging,[5] and chromatography.[6] Particular interest has grown in developing methods for the synthesis of soft nanoparticles as potential carriers for the targeted delivery and controlled release of therapeutic agents for diagnostic and treatment purposes.[7−11] Although many types of these nanoparticles have been developed, few have advanced to clinical use because of a lack of consistent toxicology data, which in turn arises partly because nanoparticle preparation techniques yield erratic results across laboratories.

Soft nanoparticles are predominantly synthesized using bulk techniques. Phospholipid-based nanoparticles are typically prepared using evaporation−rehydration or solvent-injection methods, while polymeric nanoparticles are traditionally synthesized using emulsification or solvent-evaporation methods.[12−14] The technical limitations associated with such bulk methods for synthesizing soft nanoparticles constitute a significant impediment to the realization of many of the aforementioned applications. These limitations include nanoparticle size distributions that are polydisperse, irreproducible from batch to batch, and strongly dependent on chemical formulation.[11,15] A root cause of these problems is the disparity between macroscopic control over the reaction of nanoparticle precursor solutions and the microscopic

*Corresponding author. E-mail: Jennifer.hong@nist.gov.

(1) Torchilin, V. P. Multifunctional nanocarriers. *Adv. Drug Delivery Rev.* **2006**, *58* (14), 1532−1555.
(2) Jin, T.; Pennefather, P.; Lee, P. I. Lipobeads: A hydrogel anchored lipid vesicle system. *FEBS Lett.* **1996**, *397* (1), 70−74.
(3) Agrawal, A.; Deo, R.; Wang, G. D.; Wang, M. D.; Nie, S. M. Nanometer-scale mapping and single-molecule detection with color-coded nanoparticle probes. *Proc. Natl. Acad. Sci. U.S.A.* **2008**, *105* (9), 3298−3303.
(4) Hu, Z. B.; Lu, X. H.; Gao, J.; Wang, C. J. Polymer gel nanoparticle networks. *Adv. Mater.* **2000**, *12* (16), 1173−1176.
(5) Kim, J. S.; Rieter, W. J.; Taylor, K. M. L.; An, H.; Lin, W. L.; Lin, W. B. Self-assembled hybrid nanoparticles for cancer-specific multimodal imaging. *J. Am. Chem. Soc.* **2007**, *129* (29), 8962−8963.
(6) Schillemans, J. P.; Flesch, F. M.; Hennink, W. E.; van Nostrum, C. F. Synthesis of bilayer-coated nanogels by selective cross-linking of monomers inside liposomes. *Macromolecules* **2006**, *39* (17), 5885−5890.
(7) Raemdonck, K.; Demeester, J.; De Smedt, S. Advanced nanogel engineering for drug delivery. *Soft Matter* **2009**, *5* (4), 707−715.
(8) Fenart, L.; Casanova, A.; Dehouck, B.; Duhem, C.; Slupek, S.; Cecchelli, R.; Betbeder, D. Evaluation of effect of charge and lipid coating on ability of 60-nm nanoparticles to cross an in vitro model of the blood-brain barrier. *J. Pharmacol. Exp. Ther.* **1999**, *291* (3), 1017−1022.
(9) Sanvicens, N.; Marco, M. P. Multifunctional nanoparticles - properties and prospects for their use in human medicine. *Trends Biotechnol.* **2008**, *26* (8), 425−433.
(10) Thevenot, J.; Troutier, A. L.; David, L.; Delair, T.; Ladaviere, C. Steric stabilization of lipid/polymer particle assemblies by poly(ethylene glycol)-lipids. *Biomacromolecules* **2007**, *8* (11), 3651−3660.
(11) Rondeau, E.; Cooper-White, J. J. Biopolymer microparticle and nanoparticle formation within a microfluidic device. *Langmuir* **2008**, *24* (13), 6937−6945.
(12) Ferdous, A. J.; Stembridge, N. Y.; Singh, M. Role of monensin PLGA polymer nanoparticles and liposomes as potentiator of ricin A immunotoxins in vitro. *J. Controlled Release* **1998**, *50* (1−3), 71−78.
(13) An, S. Y.; Bui, M. P. N.; Nam, Y. J.; Han, K. N.; Li, C. A.; Choo, J.; Lee, E. K.; Katoh, S.; Kumada, Y.; Seong, G. H. Preparation of monodisperse and size-controlled poly(ethylene glycol) hydrogel nanoparticles using liposome templates. *J. Colloid Interface Sci.* **2009**, *331* (1), 98−103.
(14) Kabanov, A. V.; Vinogradov, S. V. Nanogels as Pharmaceutical Carriers: Finite Networks of Infinite Capabilities. *Angew. Chem., Int. Ed.* **2009**, *48* (30), 5418−5429.
(15) Xu, Q. B.; Hashimoto, M.; Dang, T. T.; Hoare, T.; Kohane, D. S.; Whitesides, G. M.; Langer, R.; Anderson, D. G. Preparation of Monodisperse Biodegradable Polymer Microparticles Using a Microfluidic Flow-Focusing Device for Controlled Drug Delivery. *Small* **2009**, *5* (13), 1575−1581.

fluid environment which determines the formation of nanoparticles. These limitations often necessitate the use of postprocessing techniques such as high-frequency sonication, freeze−thaw cycling, or membrane extrusion to homogenize nanoparticle size and composition, which can decrease yield, increase assembly time, and be incompatible with biological applications.[6]

To address these limitations, a variety of microfluidic methods have recently been developed to synthesize soft matter nanoparticles with improved control over size distribution, as size has been determined to be a critical factor in influencing nanoparticle efficacy or toxicity for a particular application.[16−18] One such method is the use of microfluidic hydrodynamic focusing[19] to precisely control the convective-diffusive mixing of miscible liquids at nanometer length scales which determine the formation of nanoparticles. This technique has been used to direct the self-assembly of lipid molecules into nanoscale lipid vesicles of controlled size in a continuous and reproducible manner,[20] obviating the need for postprocessing to homogenize nanoparticle size. Similar microfluidic approaches have been used to produce polymeric nanoparticles.[11,21]

Beyond these single-material lipid or polymer nanoparticle systems that have been synthesized using microfluidic devices, relatively few microfluidic methods for the precisely controlled synthesis of multiple-material hybrid nanoparticle systems have been demonstrated,[22−24] despite the important applications thereof. In particular, liposome−hydrogel hybrid nanoparticles, also known as lipobeads, combine many of the advantageous material properties of the individual constituents for therapeutic applications.[2,6,13,25−27] The hydrogel interior improves both the mechanical stability of hybrid liposome−hydrogel nanoparticles and the controlled release of encapsulated therapeutic agents,

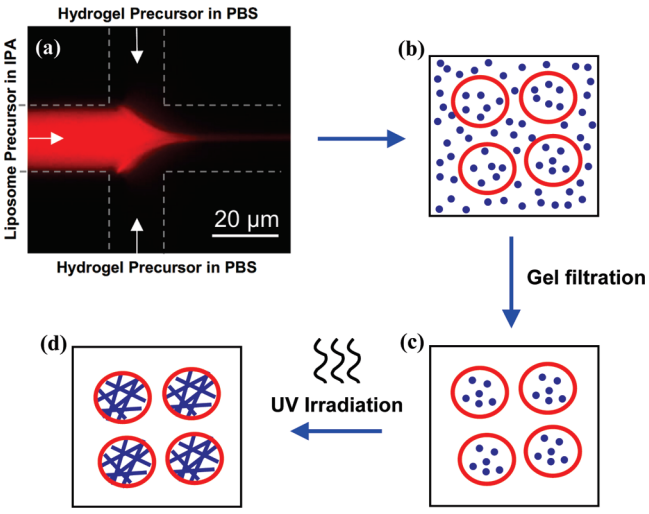

Figure 1. Schematic depicting the on-chip microfluidic directed self-assembly and off-chip polymerization of liposome−PNIPA hydrogel nanoparticles. (a) A solution of lipid and lipophilic tracer DiD (red) dissolved in IPA was hydrodynamically focused by a solution of the hydrogel precursor in buffer. Microfluidic mixing was used to direct the formation of nanoscale lipid vesicles with encapsulated gel precursors, and the sample was collected (b) at the device outlet. (c) The extravesicular gel precursor material was removed by gel filtration, and the particles were resuspended in buffer. (d) Subsequent UV irradiation initiated the free-radical polymerization of the liposome interior which produced liposome−PNIPA hydrogel nanoparticles.

while the many useful surface properties of the exterior lipid vesicle are retained for both stealth capability and targeted delivery.[13,28−32] This potential therapeutic utility motivates the development of advanced microfluidic methods to control the synthesis of these more structurally complex soft matter nanostructures.

In this Article, we present a microfluidic approach to the directed self-assembly of monodisperse liposome−hydrogel hybrid nanoparticles of controlled size. We selected poly(*N*-isopropylacrylamide) (PNIPA) as our model polymer, as it is one of the most widely studied thermoresponsive polymers for therapeutic applications and also because it has been used recently for the bulk formation of lipobeads.[26,33−35] As shown in Figure 1, our approach utilizes microfluidic hydrodynamic focusing to control the diffusive mixing of two miscible liquids[36] that separately contain the precursors to our hybrid nanoparticles. One solution contains a mixture of phospholipids and cholesterol in isopropanol (IPA) and forms the central stream in Figure 1a. The outer

(16) Jiang, W.; Kim, B. Y. S.; Rutka, J. T.; Chan, W. C. W. Nanoparticle-mediated cellular response is size-dependent. *Nature Nanotechnol.* **2008**, *3* (3), 145−150.
(17) Lewinski, N.; Colvin, V.; Drezek, R. Cytotoxicity of nanoparticles. *Small* **2008**, *4* (1), 26−49.
(18) Farokhzad, O. C.; Langer, R. Impact of Nanotechnology on Drug Delivery. *ACS Nano* **2009**, *3* (1), 16−20.
(19) Knight, J. B.; Vishwanath, A.; Brody, J. P.; Austin, R. H. Hydrodynamic focusing on a silicon chip: Mixing nanoliters in microseconds. *Phys. Rev. Lett.* **1998**, *80* (17), 3863−3866.
(20) Jahn, A.; Vreeland, W. N.; Gaitan, M.; Locascio, L. E. Controlled vesicle self-assembly in microfluidic channels with hydrodynamic focusing. *J. Am. Chem. Soc.* **2004**, *126* (9), 2674−2675.
(21) Karnik, R.; Gu, F.; Basto, P.; Cannizzaro, C.; Dean, L.; Kyei-Manu, W.; Langer, R.; Farokhzad, O. C. Microfluidic platform for controlled synthesis of polymeric nanoparticles. *Nano Lett.* **2008**, *8* (9), 2906−2912.
(22) Schabas, G.; Wang, C. W.; Oskooei, A.; Yusuf, H.; Moffitt, M. G.; Sinton, D. Formation and shear-induced processing of quantum dot colloidal assemblies in a multiphase microfluidic chip. *Langmuir* **2008**, *24* (19), 10596−10603.
(23) Schabas, G.; Yusuf, H.; Moffitt, M. G.; Sinton, D. Controlled self-assembly of quantum dots and block copolymers in a microfluidic device. *Langmuir* **2008**, *24* (3), 637−643.
(24) Valencia, P. M.; Basto, P. A.; Zhang, L.; Rhee, M.; Langer, R.; Farokhzad, O. C.; Karnik, R. Single-Step Assembly of Homogenous Lipidâ'Polymeric and Lipidâ'Quantum Dot Nanoparticles Enabled by Microfluidic Rapid Mixing. *ACS Nano* **2010**, *4* (3), 1671−1679.
(25) Wong, H. L.; Bendayan, R.; Rauth, A. M.; Wu, X. Y. Development of solid lipid nanoparticles containing lonically complexed chemotherapeutic drugs and chemosensitizers. *J. Pharm. Sci.* **2004**, *93* (8), 1993−2008.
(26) Patton, J. N.; Palmer, A. F. Photopolymerization of bovine hemoglobin entrapped nanoscale hydrogel particles within liposomal reactors for use as an artificial blood substitute. *Biomacromolecules* **2005**, *6* (1), 414−424.
(27) Liu, Y. T.; Li, K.; Pan, J.; Liu, B.; Feng, S. S. Folic acid conjugated nanoparticles of mixed lipid monolayer shell and biodegradable polymer core for targeted delivery of Docetaxel. *Biomaterials 31* (2), 330−338.
(28) Liu, J. W.; Stace-Naughton, A.; Jiang, X. M.; Brinker, C. J. Porous Nanoparticle Supported Lipid Bilayers (Protocells) as Delivery Vehicles. *J. Am. Chem. Soc.* **2009**, *131* (4), 1354−+.
(29) Hong, J. S.; Vreeland, W. N.; DePaoli Lacerda, S. H.; Locascio, L. E.; Gaitan, M.; Raghavan, S. R. Liposome-templated supramolecular assembly of responsive alginate nanogels. *Langmuir* **2008**, *24* (8), 4092−4096.
(30) Kazakov, S.; Kaholek, M.; Teraoka, I.; Levon, K. UV-induced gelation on nanometer scale using liposome reactor. *Macromolecules* **2002**, *35* (5), 1911−1920.
(31) Monshipouri, M.; Rudolph, A. S. Liposome-Encapsulated Alginate - Controlled Hydrogel Particle Formation and Release. *J. Microencapsulation* **1995**, *12* (2), 117−127.
(32) Van Thienen, T. G.; Lucas, B.; Flesch, F. M.; van Nostrum, C. F.; Demeester, J.; De Smedt, S. C. On the synthesis and characterization of biodegradable dextran nanogels with tunable degradation properties. *Macromolecules* **2005**, *38* (20), 8503−8511.
(33) Kazakov, S.; Kaholek, M.; Kudasheva, D.; Teraoka, I.; Cowman, M. K.; Levon, K. Poly(N-isopropylacrylamide-co-1-vinylimidazole) hydrogel nanoparticles prepared and hydrophobically modified in liposome reactors: Atomic force microscopy and dynamic light scattering study. *Langmuir* **2003**, *19* (19), 8086−8093.
(34) Vihola, H.; Laukkanen, A.; Valtola, L.; Tenhu, H.; Hirvonen, J. Cytotoxicity of thermosensitive polymers poly(N-isopropylacrylamide), poly(N-vinylcaprolactam) and amphiphilically modified poly(N-vinylcaprolactam). *Biomaterials* **2005**, *26* (16), 3055−3064.
(35) Kazakov, S.; Levon, K. Liposome-nanogel structures for future pharmaceutical applications. *Curr. Pharm. Des.* **2006**, *12* (36), 4713−4728.
(36) Jahn, A.; Stavis, S. M.; Hong, J. S.; Vreeland, W. N.; DeVoe, D. L.; Gaitan, M. Microfluidic Mixing and the Formation of Nanoscale Lipid Vesicles. *ACS Nano* **2010**, online.

sheath flow consists of an aqueous solution of *N*-isopropylacrylamide (NIPA), cross-linker, and free-radical initiator, in phosphate-buffered saline (PBS).

Using this approach, we can direct the assembly of liposomes at the interface between the two streams, and these liposomes encapsulate the contents of the aqueous solution, i.e., the hydrogel precursors. Moreover, by varying the volumetric flow rate ratio (VFRR) of the aqueous outer streams to the central lipid−IPA stream, the convective-diffusive mixing conditions at the interface are altered, and thereby the size of the liposomes can be controlled. The liposomes at the outlet of the microfluidic chip are then collected, purified by gel filtration, and UV-irradiated off-chip to polymerize the encapsulated precursors into a hydrogel core. Hybrid nanoparticles of controlled size can thus be prepared in the 150−300 nm diameter range with a polydispersity of $< 5\%$ (relative standard deviation). This approach may be extended to the assembly of other hybrid nanoparticle systems of interest.[37] Microfluidic assembly may offer greater control over nanoparticle size and compositional requirements as well as provide a platform that can produce multiple size distributions of nanoparticle populations from a single initial formulation.

Experimental Section[38]

Materials. The lipid dye 1,1′-dioctadecyl-3,3,3′,3′-tetramethylindodicarbocyanine perchlorate (DiD) was obtained from Molecular Probes (Eugene, OR) and 1,2-dipalmitoyl-*sn*-glycero-3-phosphocholine (DPPC) and cholesterol from Avanti Polar Lipids (Alabaster, AL). Dihexadecyl phosphate (DCP), *N*-isopropylacrylamide (NIPA) (97% purity), *N*,*N*′-methylenebis-(acrylamide) (MBA) (99% purity), 2,2-diethoxyacetophenone (DEAP) (purum >95% GC), and sodium azide (NaN_3) were obtained from Sigma-Aldrich. Polydimethylsiloxane (PDMS) (Sylgard 184) was purchased from Dow Corning. Hamilton gastight glass syringes and anotop syringe filters were obtained from Fisher Scientific. D-Salt columns were purchased from Pierce (Rockford, IL).

Microfluidic Device Fabrication. A schematic and bright-field micrograph of the microfluidic device is shown in Figure 2. Microfluidic devices were constructed using standard photolithographic microfabrication processes. A thin film of positive tone photoresist was spin-coated onto the front side of a double-side-polished silicon substrate wafer with a thickness of ≈290 μm. Networks of fluidic channels with widths of 21 ± 1 μm (mean ± expanded uncertainty) were patterned in the photoresist using contact photolithography. Device patterns were transferred into the substrate using Bosch process deep reactive ion etching to a depth of 39 ± 1 μm (mean ± expanded uncertainty). A thin film of silicon dioxide was deposited as an etch stop on the front side of the substrate using plasma-enhanced chemical vapor deposition. A thin film of positive tone photoresist was spin-coated onto the back side of the substrate, and a second layer of contact photolithography was used to pattern access holes aligned to the channel inlets and outlets. Access holes were then formed by deep reactive ion etching of the substrate through to the etch stop. The substrate wafer was immersed in buffered hydrofluoric acid to remove the silicon dioxide etch stop and finally cleaned with a mixture of ammonium hydroxide:hydrogen peroxide:water (≈5:1:1 volume ratio) at a temperature of ≈80 °C. A borosilicate glass cover wafer with a thickness of ≈170 μm was anodically bonded to the front side of the substrate wafer to form enclosed

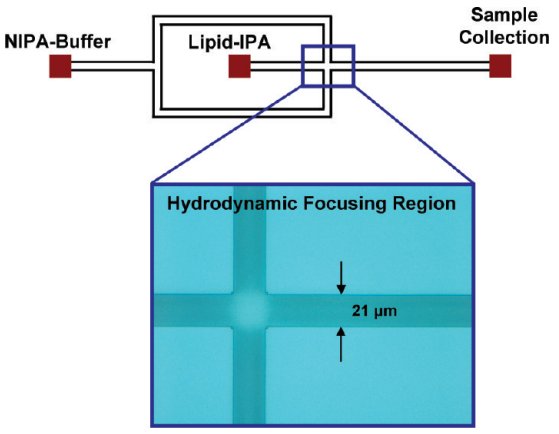

Figure 2. Device schematic and optical micrograph of the microfluidic hydrodynamic focusing cross junction. Microchannels were fabricated in a silicon substrate which was anodically bonded to a borosilicate glass cover. The microfluidic channel was 21 ± 1 μm wide and 39 ± 1 μm deep (mean ± expanded uncertainty).

microfluidic channels. Fluidic connectors were adhered to the backside of the substrate wafer to couple poly(ether ether ketone) capillaries to the inlets and outlets of the microfluidic devices. The opposing end of each inlet capillary was attached to a gastight glass Hamilton syringe filled with reagent. The syringes were mounted onto syringe pumps (Harvard Apparatus, MA) to control continuous fluid flow into the microchannels.

Epifluorescence Microscopy. An inverted optical microscope was used in epifluorescence mode to observe microfluidic formation of nanostructures. Microfluidic flow was imaged through the cover wafer with a plan apochromat air immersion objective of magnification 40× and numerical aperture 0.95. A metal halide arc lamp was used with a 625 to 655 nm band-pass filter for fluorescence excitation, and fluorescence emission was isolated with a 660 nm dichroic mirror and refined with a 665−715 nm band-pass filter. Videos and images were acquired with either an electron multiplying or color charge coupled device camera. Following nanoparticle synthesis experiments, hybrid nanoparticles were suspended on a glass coverslip with a thickness of ≈170 μm for inspection using the same optical setup.

Buffer Preparation. 0.01 mmol/L phosphate buffered saline (PBS) (0.138 mol/L NaCl, 2.7 mmol/L KCl, pH 7.4) was used in all experiments unless otherwise specified. PBS was prepared in 18.2 MΩ filtered deionized water with the addition of 3 mmol/L NaN_3 to prevent bacterial growth. All PBS solutions were filtered through a 0.1 μm syringe filter prior to use in sample preparation.

Lipid and Hydrogel Precursor Preparation. A mixture of DPPC:cholesterol:DCP (7:2:1 molar ratio) and 0.5 mol fraction % DiD lipophilic tracer was used in the formation of the empty liposomes and liposome−hydrogel hybrid nanoparticles. The mixture was dissolved in chloroform in a glass scintillation vial and was dried down under dry nitrogen for 45 min to produce a thin lipid film, and the dried lipid film was placed in a vacuum desiccator overnight to remove any residual solvent. The NIPA:MBA:DEAP (3.5%:0.35%:0.1% weight per volume ratio) gel precursor solution was prepared in PBS. An Omnicure S2000 (EXFO Life Sciences, Canada) lamp (λ = 365 nm; 40 W cm^{-2}) was used to initiate free-radical polymerization of the bulk hydrogel precursor material. The onset of polymerization was observed immediately upon UV irradiation, and complete bulk gel formation was verified after 15 min of irradiation.

Precursors to Hybrid Nanoparticles by Microfluidic Flow Focusing. Nanoscale liposomes containing hydrogel precursors were synthesized using microfluidic mixing controlled by hydrodynamic focusing.[36] The lipid film was redissolved in dry 0.1 μm filtered IPA to obtain a 6.25 mmol/L solution. The lipid solution and either the gel precursor (experimental) or PBS (control)

(37) Hamidi, M.; Azadi, A.; Rafiei, P. Hydrogel nanoparticles in drug delivery. *Adv. Drug Delivery Rev.* **2008**, *60* (15), 1638−1649.

(38) Certain commercial materials and equipment and identified in order to specify adequately experimental procedures. In no case does such identification imply recommendation or endorsement by the Nationals Institute of Standards and Technology, not does it imply that the items identified are necessarily the best available for the purpose.

solution were each loaded in a glass syringe and connected to the device inlets, as shown in Figure 2. Syringe pumps were used to control the flow of lipid−IPA solution into the center channel and PBS or gel precursor solution into the side channels to hydrodynamically focus the lipid−IPA stream, shown in Figure 1a. Empty liposomes were formed in PBS at VFRRs of 10:1, 15:1, 20:1, and 25:1, while liposomes encapsulating the gel precursor were formed at VFRRs of 10:1, 15:1, and 25:1. The total volumetric flow rate (Q_T) and the average fluid flow velocity (v) were held constant at 9.6 μL/min and 0.2 m/s, respectively, at all times. This resulted in an operating Re range of approximately 2−5, which is well within the limit of laminar fluid flow.

Off-Chip Formation of Hybrid Nanoparticles. Liposomes encapsulating the gel precursor were passed through a D-Salt polyacrylamide column (6 kDa cutoff), using PBS as the elution buffer, to remove the extravesicular gel precursor material from the sample. PDMS wells (1.6 cm diameter × 0.3 cm height) were stamped and cut from a cured PDMS sheet, and the wells were cleaned with ethanol followed by deionized water. They were dried with nitrogen before being placed on a glass microscope slide. Added to each well were 0.5 mL aliquots of sample, which were then irradiated with UV light at 365 nm from the Omnicure S2000 for 15 min.

Asymmetric Flow Field-Flow Fractionation and Multiangle Laser Light Scattering (AF4-MALLS). An Eclipse AF4-MALLS instrument was used for size fractionation and characterization of the liposomes and nanoparticles. The AF4 separation channel had a 190 μm spacer, and a regenerated cellulose membrane with a 10 kDa cutoff was used for the cross-flow partition. For the control liposomes, 10 mmol/L PBS was used as the carrier solution. 10 μL of the liposome solution was loaded into the AF4 injection loop, and the fractionation was conducted with a 1 mL/min channel flow and a 0.8 mL/min to 0.0 mL/min linearly decreasing cross-flow gradient over 70 min. For the hybrid nanoparticles, a 5 mmol/L PBS carrier solution, a 50 μL sample injection, and a 0.6 to 0.0 mL/min linearly decreasing cross-flow gradient over a 35 min elution period were used. MALLS data were collected simultaneously at 10 scattering angles on the eluting sample. A coated sphere model[39] was applied to the data using an estimated bilayer thickness of 5 nm to determine the geometric radii distributions of liposomes and hybrid nanoparticles.

Dynamic Light Scattering (DLS). A 90Plus/BI-MAS particle size analyzer instrument was used for DLS measurements (Brookhaven Instruments). The instrument was equipped with a 15 mW solid state laser with a wavelength of 659 nm, and measurements were made at 90° at a rate of one measurement per second. Nanoparticle samples were centrifuged at 10 000 rpm for 4 min to remove any dust or aggregates prior to measurement. The supernatant was then aspirated and diluted 1:10 in 0.02 μm filtered PBS, and the sample was added to a poly(methyl methacrylate) cuvette and placed in the measurement cell. Measurements were made over a series of temperatures.

Transmission Electron Microscopy (TEM). TEM of the hybrid nanoparticles was performed on a Philips EM 400T microscope operating at 120 kV equipped with a Soft Imaging System CCD camera (Cantega 2K). TEM samples were prepared by dropping diluted solutions onto 400-mesh carbon-coated copper grids (from Ted Pella) and briefly air-drying the samples prior to measurements.

Results and Discussion

Empty Liposomes in PBS. Empty liposomes, prepared in PBS without the hydrogel precursor, were synthesized in the microfluidic device as a calibration to determine the size ranges achieved at varying volumetric flow-rate ratios (VFRRs) with our device geometry and lipid formulation. Under the laminar flow conditions typical at microfluidic length scales, the mixing of miscible liquids flowing in parallel streams occurs predominantly by molecular diffusion, as influenced by convection in our system. In both the hydrodynamic focusing region and in the downstream mixing channel, IPA diffused into the buffer and vice versa to the point where the concentration of lipid exceeded its critical micelle concentration and caused the lipids to self-assemble into vesicle bilayers, thus shielding the hydrophobic moieties from water. As the liposomes self-assembled, the vesicles encapsulated the surrounding buffer or hydrogel precursor mixture into the aqueous vesicle core.

The critical mixing time over which this self-assembly process occurred was dependent on the extent of focusing of the center stream.[36] At lower focusing, or smaller VFRRs, the center lipid−IPA stream was relatively wide with a low surface-to-volume ratio between the lipid stream and sheath flows, requiring a longer diffusive mixing time to deplete the center stream. The prolonged lipid solubility resulted in the self-assembly of larger vesicles further downstream in the diffusive mixing channel while fewer vesicles formed in the focusing region. At higher focusing, or larger VFRRs, convective flow resulted in a relatively narrow center stream, which reduced the diffusion distance and increased diffusive mixing in the hydrodynamic focusing region. Higher focusing also resulted in a higher surface-to-volume ratio and a faster depletion of the center stream. This caused the self-assembly of smaller liposomes predominantly within the hydrodynamic focusing region as opposed to downstream in the mixing channel. Control of these flow conditions enabled predictable and repeatable steady-state mixing and the continuous production of liposome and precursor hybrid nanoparticle size distributions.

The liposomes were formed at VFRRs of 10:1, 15:1, 20:1, and 25:1, and the collected samples were characterized by AF4-MALLS. The size distribution of each VFRR sample is shown in Figure 3a. Here, for a given sample, each data point represents a MALLS measurement of a size-fractionated component; thereby, the overall size distribution is a more accurate characterization of the sample compared to that obtained from traditional static or dynamic light scattering.[40] The size distributions show the expected trend where an increase in VFRR results in a smaller size distribution of liposomes.[41] For a simplified view of this trend, Figure 3b plots the average radius and polydispersity vs VFRR. In calculating these averages, the sizes were weighted by the number density data from Figure 3a. The average radius and standard deviation of the distributions for the 10:1, 15:1, 20:1, and 25:1 samples were 65 ± 6, 49 ± 7, 44 ± 6, and 41 ± 6 nm, respectively. These numbers indicate that each liposome population is narrowly dispersed, particularly when compared to other liposome preparation techniques.[36] At VFRRs 20:1 and 25:1, the size varies only slightly, suggesting that we are approaching the lower limit of liposome size that can be produced for this formulation in our microfluidic device. These results guided our selection of VFRR settings for the formation of the liposome−PNIPA hybrid nanoparticles.

Liposome−PNIPA Hybrid Nanoparticles. Because of the incremental difference in average vesicle size from the empty liposome synthesis experiments between VFRRs 15:1 and 20:1, and more so between 20:1 and 25:1, the 20:1 VFRR was omitted

(39) Korgel, B. A.; van Zanten, J. H.; Monbouquette, H. G. Vesicle size distributions measured by flow field-flow fractionation coupled with multiangle light scattering. *Biophys. J.* **1998**, *74* (6), 3264−3272.

(40) Wyatt, P. J. Submicrometer particle sizing by multiangle light scattering following fractionation. *J. Colloid Interface Sci.* **1998**, *197* (1), 9−20.

(41) Jahn, A.; Vreeland, W. N.; DeVoe, D. L.; Locascio, L. E.; Gaitan, M. Microfluidic directed formation of liposomes of controlled size. *Langmuir* **2007**, *23* (11), 6289−6293.

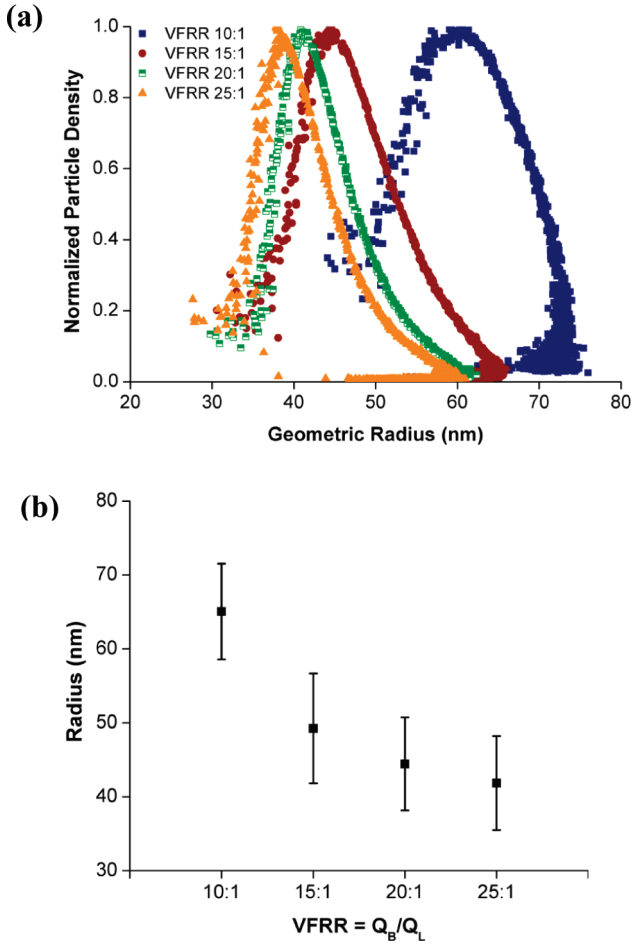

Figure 3. (a) Size distributions measured by AF4-MALLS of empty liposome populations formed in PBS alone by hydrodynamic focusing at varying VFRRs. (b) Average outer vesicle radius and standard deviation of each population are shown. Q_B and Q_L denote the volumetric flow rates of the buffer and lipid−IPA, respectively.

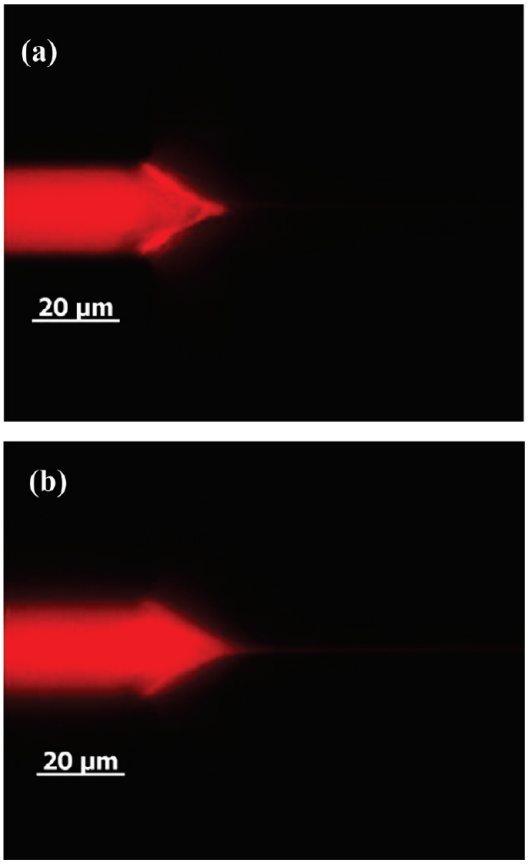

Figure 4. Transient phase separation observed at the hydrodynamic focusing interface at (a) the bottom of the microfluidic channel near the glass surface of the device and (b) in the middle of the microfluidic channel.

from the hybrid nanoparticle formation run. Liposomes encapsulating the NIPA:MBA:DEAP hydrogel precursor solution were formed in a single continuous-flow run at VFRRs of 10:1, 15:1, and 25:1.

Compared to the formation of the liposomes in PBS alone, transient chemical interactions arising from phase separation of the precursor components occurred more frequently at the hydrodynamic interface between the lipid and hydrogel precursor streams, especially closer to the borosilicate glass surface of the device (Figure 4). Such interfacial buildup occurred at all three VFRR formation settings but did not disrupt the directed assembly of precursor hybrid nanoparticles. This issue was more problematic in trials with significantly higher hydrogel precursor concentration (data not shown), however, providing some insight into the limitations of our technique.

The liposomes collected at the outlet of the microfluidic chip were purified by gel filtration and then UV polymerized to yield liposome−PNIPA hybrid nanoparticles (Figure 1). The size distributions of these nanoparticle samples were then measured by AF4-MALLS and are shown in Figure 5. The liposomes containing NIPA before UV irradiation were also characterized, and those results (Figure 5a) indicate structures with low polydispersities comparable to the empty liposomes. Polymerization did not alter the average size appreciably, and the final liposome−PNIPA hybrid nanogels had even narrower size distributions, as shown in Figure 5b. This held true at each of the applied VFRRs, spanning an overall size range of about 150−300 nm in diameter. The average radius and polydispersity for each VFRR is shown is Figure 4c; these were 142 ± 4, 109 ± 3, and 92 ± 5 nm for VFRRs of 10:1, 15:1, and 25:1, respectively.

An interesting point is that, at a given VFRR, liposomes containing the NIPA precursor mixture were approximately twice the size of empty liposomes (compare Figures 3a and 5a). AF4-MALLS measurements confirmed that the size distributions of the liposomes containing NIPA precursor before and after the polyacrylamide gel filtration step were the same (data not shown). The similarity in size distributions in Figure 5a,b indicates that this discrepancy from the empty liposomes size distributions was not caused by the gel filtration or UV polymerization but was rather a result of changes in the microfluidic chemical environment caused by the addition of the hydrogel precursor molecules in the aqueous stream. These changes evidently altered the steric and/or chemical conditions of the molecular self-assembly and encapsulation processes. The interfacial buildup in the presence of NIPA may have also played a role in this context.

The formation of liposome−PNIPA nanoparticles by our approach showed a batch-to-batch reproducibility in size to within 5−15% as measured by AF4-MALLS. This variability was attributed to experimental variation in convective flow conditions as well as the transient chemical interactions observed between the hydrogel and liposome precursor streams during the continuous formation of precursor hybrid nanoparticle samples.

The hybrid nanoparticles were also characterized qualitatively by TEM (Figure 6). Each sample was air-dried on a TEM grid

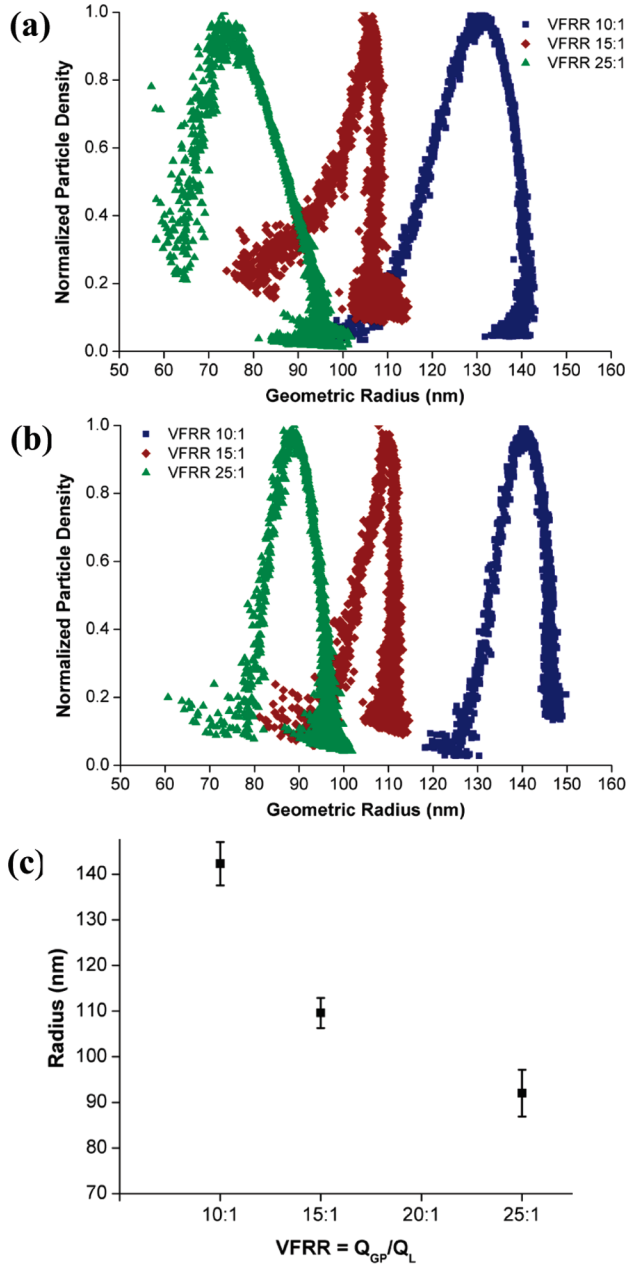

Figure 5. (a) Size distributions of lipid−NIPA liposomes and (b) liposome−PNIPA hybrid nanoparticles formed by polymerizing the liposomes in (a). (c) Average liposome−PNIPA hybrid nanoparticle size at varying VFRRs. Q_{GP} and Q_L denote the flow rates of the gel precursor and lipid solutions, respectively. The small standard deviation for each population illustrates the narrow size distributions achieved by our microfluidic directed self-assembly method.

prior to imaging, and the micrographs in Figure 6 therefore correspond to dehydrated nanoparticles. The hybrid nanoparticles were uniformly solid and exhibited the round shape of the liposome envelope, which confirms the successful encapsulation and polymerization of the hydrogel precursor within the liposomal interior. The particle size exhibits a decrease with an increase in VFRR, as earlier demonstrated by AF4-MALLS. Note that the sizes are much smaller than those shown in Figure 5, which is attributed to the dehydration of the liposome−PNIPA nanoparticles.

Temperature Sensitivity of Liposome−PNIPA Nanoparticles. To further validate the solid core composition of the liposome−PNIPA nanoparticles produced by our microfluidic synthesis strategy, we investigated the temperature sensitivity of particles synthesized at a VFRR of 10:1 using DLS. It is known that PNIPA exhibits a lower critical solution temperature (LCST) in water, and as a result, PNIPA hydrogels shrink when heated up to its LCST, which is ≈32 °C.[42,43] Therefore, we measured the size of liposome−PNIPA hydrogel nanoparticles over a range from 25 to 32 °C, and then at 37 °C, which is the physiological temperature at which these nanoparticles may potentially be applied. At each temperature, the sample was equilibrated, and three measurement runs were performed. The average values of the hydrodynamic diameter D_h from DLS along with the standard deviations are plotted in Figure 7. The average D_h was 260 ± 10 nm at 25 °C, 243 ± 7 nm at 32 °C, and at 37 °C was 224 ± 7 nm. These results show the characteristic temperature response of PNIPA, with the size decreasing past the LCST (32 °C). Similar results have been reported for liposome−PNIPA hybrid particles prepared by a bulk method.[35]

Another interesting phenomenon is the effect of prolonged exposure at 37 °C on liposome−PNIPA hydrogel nanoparticles. Corresponding size data from DLS are shown in Figure 8. Each data point corresponds to the average D_h and standard variation from a 2.5 min measurement run. After 7.5 min exposure at 37 °C, the average D_h increased significantly, which is indicative of nanoparticle aggregation. Similar behavior has also been previously reported[35] for bulk-prepared liposome−PNIPA particles. The increasing hydrophobicity of the PNIPA gel cores is believed to drive such aggregation.

Stability of Liposome−PNIPA Nanoparticles. Liposome−PNIPA nanoparticles were monitored for stability after formation. Fluorescence micrographs of particles 2 weeks after formation (Figure 9a) confirm that the particles are not highly aggregated. TEM measurements in Figure 9b show hybrid nanoparticles made at a VFRR 15:1 after 2 months. The nanoparticles generally show the same solid, spherical structure as the initially polymerized sample shown in Figure 6b, further confirming the stability and robustness of the nanoparticles. DLS measurements made on samples after 4 months also verified that the sizes remained consistent, which is likely due to the lipid bilayer coating preventing aggregation of the PNIPA nanogel cores. It should be noted that the DCP component of the lipid formulation has a negative charge, which confers electrostatic stability to the resulting liposomes as well as to the liposome−PNIPA nanoparticles.

Bulk preparations of lipid−hydrogel nanoparticles typically involve the use of a single formulation of lipid and hydrogel precursor to produce a single vesicle population with a particular size distribution determined by the application of several size-altering postprocessing steps, which can decrease yield, increase preparation time, and introduce biological compatibility issues. Using our microfluidic method, we synthesized relatively monodisperse populations of liposome−PNIPA hybrid nanoparticles from a single formulation without size-altering postprocessing. Through precise variation of microfluidic mixing conditions, our method should be able to produce nanoparticle populations with any intended average size within some finite range from an initial formulation, limited primarily by the chemical compatibility of the nanoparticle precursor solutions at the fluidic interface. Our

(42) Liu, Q. F.; Zhang, P.; Qing, A. X.; Lan, Y. X.; Lu, M. G. Poly(N-isopropylacrylamide) hydrogels with improved shrinking kinetics by RAFT polymerization. *Polymer* **2006**, *47* (7), 2330−2336.
(43) Kratz, K.; Hellweg, T.; Eimer, W. Structural changes in PNIPAM microgel particles as seen by SANS, DLS, and EM techniques. *Polymer* **2001**, *42* (15), 6631−6639.

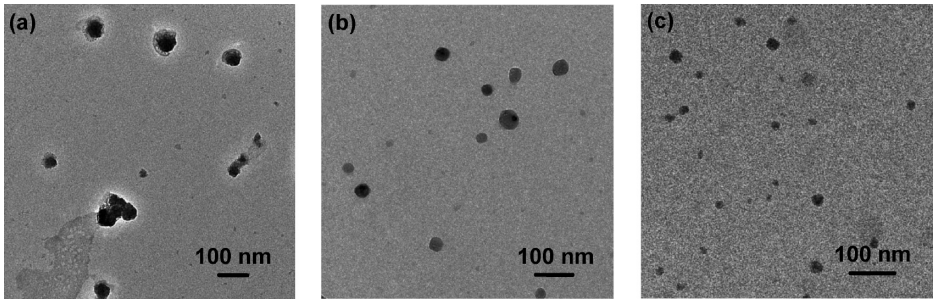

Figure 6. TEM micrographs of liposome−PNIPA hybrid nanoparticles formed at varying VFRRs of (a) 10:1, (b) 15:1, and (c) 25:1. The nanoparticles exhibit characteristics of solid spherical structures and show a trend of decreasing size with increasing VFRR.

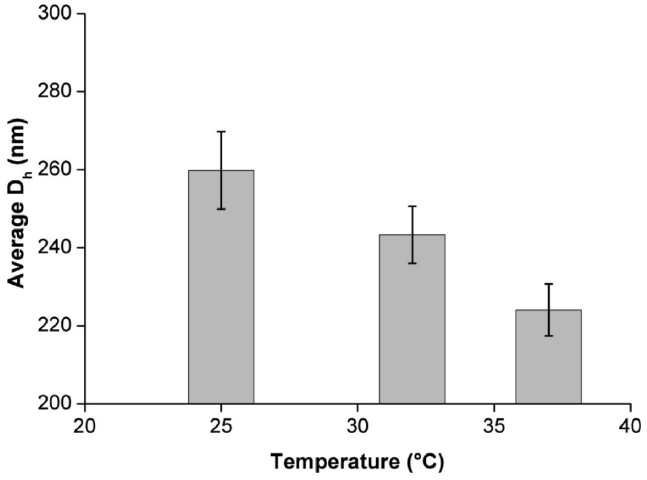

Figure 7. DLS data showing the effect of increasing temperature on the hydrodynamic diameter D_h of liposome−PNIPA hybrid nanoparticles prepared at a VFRR of 10:1.

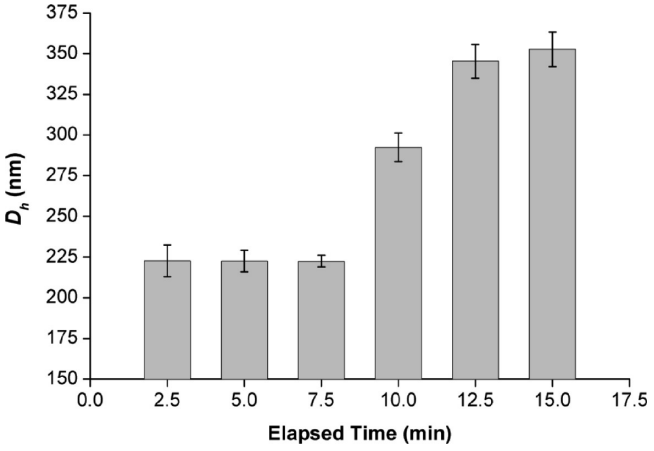

Figure 8. Time-lapse DLS data showing the effect of prolonged exposure to 37 °C on the hydrodynamic diameter D_h of liposome−PNIPA nanoparticles (VFRR of 10:1).

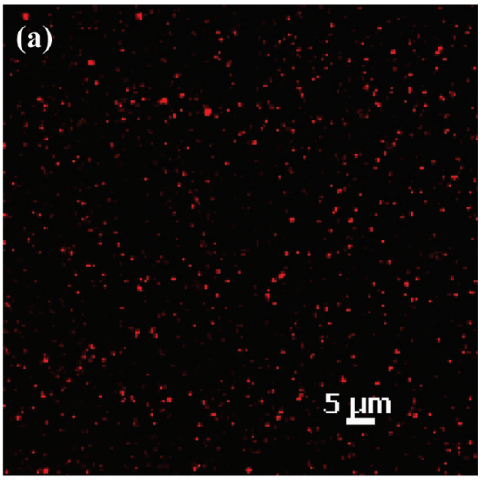

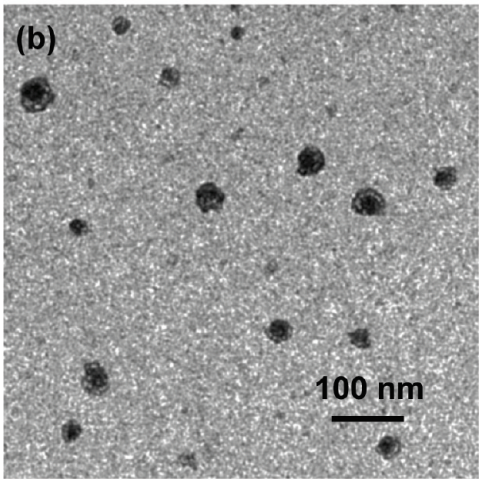

Figure 9. Stability of the liposome−PNIPA hybrid nanoparticles: (a) Epifluorescence micrograph taken 2 weeks after sample formation shows that the nanoparticles are not highly aggregated. (b) TEM of the VFRR 15:1 sample 2 months after formation shows that the particles still retain similar structure and size, comparable to the original sample in Figure 6b.

approach could be useful in therapeutic agent delivery and cellular uptake applications, which often require different carrier materials and specific sizes to target different types of cells. For these applications, it may be necessary to remove residual IPA by dialysis following nanoparticle synthesis to prevent potentially toxic effects. With the many polymers and lipids commercially available and the interest in tailoring different types of nanoparticles for various applications,[44] the development of a more controlled and standardized formation method such as the presented model system would be advantageous. We expect that this system could be adapted and optimized for the microfluidic-directed synthesis of hybrid nanoparticles derived from other soft matter precursors of present interest.[35]

(44) Moghimi, S. M.; Hunter, A. C.; Murray, J. C. Long-circulating and target-specific nanoparticles: Theory to practice. *Pharmacol. Rev.* **2001**, *53* (2), 283−318.

Conclusion

We have demonstrated a microfluidic method to direct the assembly of liposome−poly(*N*-isopropylacrylamide) (PNIPA) hybrid nanoparticles. By varying microfluidic mixing conditions, we were able to control the size of the liposome molds that encapsulated the gel precursor, which thereby determined the sizes of the resultant hybrid nanoparticles. Using light scattering and TEM, we verified that our method produced narrowly dispersed populations of lipid−hydrogel hybrid nanoparticles over a size range pertinent to targeted delivery and controlled release applications. We believe that this microfluidic approach may be customized for the synthesis of a wide variety of soft nanoparticles that are currently prepared via bulk methods. Our method can be further improved through on-chip integration of the off-chip formation steps; however, the main objective of our work is to demonstrate the utility of a microfluidic-directed approach toward hybrid nanoparticles. Future work must also assess the encapsulation efficiency and stability of hybrid nanoparticles with regard to clinical application.

Acknowledgment. This research was performed while SMS held a National Research Council Research Associateship Award at the National Institute of Standards and Technology (NIST). Device fabrication was performed in part at the Cornell Nanoscale Science and Technology Facility (CNF), a member of the National Nanotechnology Infrastructure Network supported by the NSF, and in part at the NIST Center for Nanoscale Science and Technology (CNST). The authors thank the CNF and CNST staff for assistance with device fabrication, Wyatt Vreeland from the NIST Biochemical Science Division for use of the AF4-MALLS instrumentation, and Jon Geist and Darwin Reyes from the NIST Semiconductor Electronics Division for helpful discussions.